DOI: 10.1002/ejic.200600424

Pentacoordination at Germanium by Transannular Bonding of Sulfur or Oxygen in an Eight-Membered Ring: An Experimental and Theoretical Study

Simplicio González-Montiel,[a] Noemí Andrade-López,[a] Verónica García-Montalvo,[b] Juan Antonio Cogordan,[b] and José G. Alvarado-Rodríguez*[a]

Keywords: Germanium / Hypercoordinate compounds / Structure elucidation / Density functional theory / NBO analysis

Treatment of L_nGeCl_{4-n} with $D(C_6H_4SH)_2$ in the presence of *n*BuLi leads to the formation of the stable compounds $D(C_6H_4S)_2GeL_1L_2$ (for D = S, L_1 = Cl, L_2 = Ph, **1** and $L_1 = L_2$ = Ph, **3**; for D = O, L_1 = Cl, L_2 = Et, **4** and $L_1 = L_2$ = Ph, **5**). The $S(C_6H_4S)_2Ge(Ph)Br$ compound (**2**) has been synthesised by halogen exchange from **1** and potassium bromide. X-ray structure determinations of complexes **1**–**5** reveal that the germanium atom acts as an acceptor atom displaying an intramolecular transannular interaction with the chalcogen D atom. The geometry of the pentacoordinate Ge atom in the title compounds is described as distorted trigonal bipyramidal with a 64–31 % distortion displacement. The D→Ge (D = S, O) hypercoordinate interaction was studied by DFT methods using correlation consistent basis sets and relativistic ECP for Ge. NBO analysis showed that this interaction can be explained in terms of the interplay of covalent and Coulombic interactions.

Introduction

In order to gain a deeper insight into the nature of the secondary bonding[1] and its relation with the hypercoordination phenomena of group 14 and 15 elements, a large variety of metallocanes of type **I** $D(CH_2CH_2E)_2A$ (D = NR′, O, S; E = O, S, CH_2; A = Ge, Sn, Pb, As, Sb or Bi) have been prepared and structurally characterised (Scheme 1).[2–8] In the solid state metallocanes usually exhibit a strong 1,5-transannular interaction between a Lewis acidic acceptor A and a basic donor D atom (D→A), where the coordination mode of the ligand $D(CH_2CH_2E)_2^{2-}$ is formally tridentate, leading to an increase in the coordination number of A. In these compounds the richness of the conformational diversity in the solid state and solution is supported by a wide variety of molecular structural features, for example bond lengths, bond angles, torsion angles and the central eight-membered ring conformation, as well as intermolecular interactions in the crystal.[2]

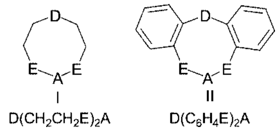

Scheme 1.

Crystallographic X-ray studies of the more constrained tricyclic systems of type **II**, known as dibenzometallocines $D(C_6H_4E)_2A$ (Scheme 1), have also shown a 1,5-transannular interaction. These compounds have been long studied in particular where D = S, E = O and A is a d block or light p block element (mainly phosphorus and silicon), meanwhile, with a softer donor atom such as D = E = S the chemistry is fully dominated by the d block metals.[9] In these transition metal complexes the transannular distance between the acidic metal centre and the thioether-like sulfur is usually quite short, suggesting the large capabilities of the $S(C_6H_4S)_2^{2-}$ as a tridentate ligand.

We have studied some monohalogenated dibenzometallocines $D(C_6H_4S)_2AHal$ (for A = Sb[5], D = S, Hal = Cl, Br, I; D = O, Hal = Cl; for A = As[10], D = S, Hal = Cl, Br, I) and have shown by means of X-ray crystallographic studies (and also DFT studies in the case of antimony) the acidic behaviour of the central atom, where the A acceptor experiences a structural change from pyramidal tricoordinate to *ψ*-trigonal-bipyramidal tetracoordinate. These results prompted us to extend the chemistry of the ligand $S(C_6H_4S)_2^{2-}$ to other p block heavier elements such as germanium(IV), where structural studies with similar ligands are scarce[11–14] and have mainly focused on metallocanes.[2–4]

Here we report an experimental and theoretical study of type **II** complexes with germanium as the acceptor atom. These compounds are good models for further understand-

---

[a] Centro de Investigaciones Químicas, Universidad Autónoma del Estado de Hidalgo,
Km. 4.5 Carretera Pachuca-Tulancingo, Pachuca, Hidalgo, C. P. 42076, México
E-mail: jgar@uaeh.edu.mx
[b] Instituto de Química, Universidad Nacional Autónoma de México, Circuito Exterior, Ciudad Universitaria,
D. F. México, C. P. 04510, México

ing the nature of the D→Ge interaction. After the description of the synthesis of dibenzogermocines and the NMR spectroscopic and X-ray crystallographic data a theoretical study is presented and discussed.

Results and Discussion

Synthesis

The ligands $S(C_6H_4SH)_2$ and $O(C_6H_4SH)_2$ were prepared following the reported method.[9,15] The reaction of the corresponding organylgermanium(IV) in THF at 0 °C with the dilithium salt of the ligand, generated in situ from the dithiol and 2 equiv. of *n*BuLi, yielded the corresponding Ge^{IV} complex (see Exp. Sect. for details). Treatment of $S(C_6H_4SLi)_2$ with $PhGeCl_3$ and Ph_2GeCl_2 yielded $S(C_6H_4S)_2GePhCl$ (**1**) and $S(C_6H_4S)_2GePh_2$ (**3**), respectively. $S(C_6H_4S)_2GePhBr$ (**2**) was synthesised from **1** by the treatment of excess KBr in a refluxing HBr/benzene mixture, giving **2** as colourless crystals. Treatment of $O(C_6H_4SLi)_2$ with $EtGeCl_3$ and Ph_2GeCl_2 yielded $O(C_6H_4S)_2GeEtCl$ (**4**) and $O(C_6H_4S)_2GePh_2$ (**5**), respectively (see Scheme 2).

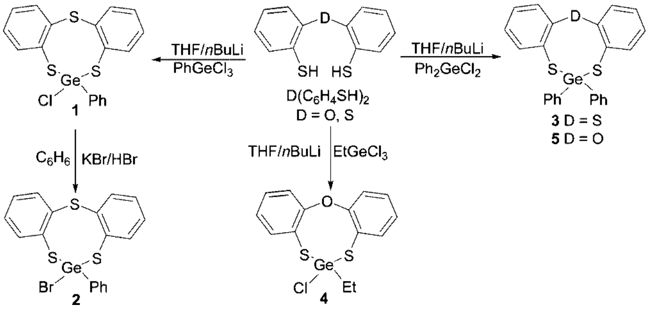

Scheme 2.

All complexes are air-stable, soluble in benzene, toluene, dichloromethane and chloroform, and insoluble in pentane, hexane and 2-propanol.

Mass Spectra

FAB mass spectra for **1**, **2**, **3** and **5** and electron impact mass spectra for **4** exhibit a low intensity ion with the appropriate isotopic ratio representing the molecular ion ($M^{\cdot+}$); in all cases a basis peak corresponding to the fragment M–L [L = Cl (**1**), Br (**2**), Ph (**3** and **5**), Et (**4**)] is observed and assigned to the $D(C_6H_4S)_2GeL$ [L = Ph (**1**, **2**, **3** and **5**), and Cl (**4**)] tricyclic moiety, confirming the binding of germanium to the sulfur thiolate-like atoms. There are peaks corresponding to the $D(C_6H_4)_2S$ moiety [D = S (**1**, **2**, **3**); O (**4**, **5**)] in all the spectra. In the case of the diphenyl germanium complexes **3** and **5** the cluster peak at 229 *m*/*z* is assigned to the protonated $GePh_2$ fragment. No more peaks could be assigned.

NMR Spectroscopy

NMR spectra of complexes **1**–**5** were recorded in a $CDCl_3$ solution at room temperature. Chemical shifts are relative to TMS. The assignments of these complexes were carried out by heteronuclear and homonuclear correlation two-dimensional experiments (HETCOR, COLOC and COSY).

^1H NMR spectra for complexes **1**–**5** each show four signals for the DC_6H_4SGe moiety in an ABCD pattern, Table 1. In solution the two DC_6H_4SGe halves are equivalent (see Scheme 3). In all complexes, the *ortho* proton 1-H is shifted towards high frequencies with respect to the free

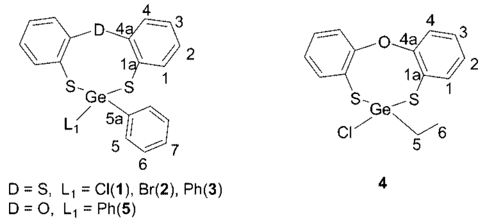

Scheme 3.

Table 1. ^1H NMR chemical shifts (δ values [ppm]) for **1**–**5** in $CDCl_3$ at 25 °C.

Compound	D	L_1	1-H	2-H	3-H	4-H	5-H	6-H	7-H
1	S	Cl	7.65	7.27	7.16	7.44	7.81	7.40	7.40
2	S	Br	7.65	7.28	7.16	7.44	7.78	7.39	7.39
3	S	Ph	7.66	7.13	7.18	7.44	7.63	7.34	7.34
4	O	Cl	7.53	7.23	7.15	7.13	1.80	1.18	–
5	O	Ph	7.56	7.09	7.04	6.85	7.65	7.32	7.32

Table 2. ^{13}C NMR chemical shifts (δ values [ppm]) for **1**–**5** in $CDCl_3$ at 25 °C.

Compound	D	L_1	C-1	C-2	C-3	C-4	C-1a	C-4a	C-5	C-5a	C-6	C-7
1	S	Cl	131.2	129.9	127.5	134.2	132.3	140.7	131.2	141.4	128.9	130.9
2	S	Br	131.2	129.9	127.5	134.3	132.3	140.7	131.1	141.9	128.9	132.1
3	S	Ph	134.3	127.4	128.3	134.9	137.4	139.8	133.2	138.2	128.5	130.0
4	O	Cl	132.6	127.7	125.8	120.2	126.2	152.7	23.1	–	8.3	–
5	O	Ph	133.7	127.5	124.6	120.6	126.6	154.8	133.6	136.4	128.4	130.1

neutral ligands.[9,15] In **4** and **5** the *ortho* proton, 4-H, is also observed at higher frequencies.

Proton decoupled ^{13}C spectra of complexes **1**–**3** and **5** display ten signals in the aromatic region, Table 2. In **4** the ethyl group is observed at low frequencies (23.1 and 8.3 ppm). In complexes **1**–**5** the values obtained for the variation of the chemical shift ($\Delta\delta$) with respect to the starting materials (free ligands and organogermanium chlorides) show the ipso carbon C-4a and the carbon C-4 at high frequencies; in these compounds the **1**–**3** complexes present large values of $\Delta\delta$. The $\Delta\delta$ value for the C-4a and C-4 in **1** are 8.2 and 4.0 ppm; in **2** they are 8.2 and 4.1 ppm; in **3** they are 7.3 and 4.7 ppm; in **4** they are 0.6 and 1.6 and in **5** they are 2.7 and 2.0 ppm, respectively. In the double phenylated **3** and **5** complexes the $\Delta\delta$ for the ipso carbon C5a presented the smallest values when compared to the diphenylgermanium dichloride (δ =3.7 ppm in **3** and 1.9 ppm in **5**). The data obtained suggest that the D→Ge transannular interaction in the complexes **3** and **5** is either very weak or completely lacking in solution.

X-ray Structures of Compounds 1–5

The molecular structures in the crystalline solid state of **1**–**5** were determined by single-crystal X-ray diffraction analyses. The ORTEP drawings are depicted in Figure 1 and selected bond lengths, angles and torsion angles are

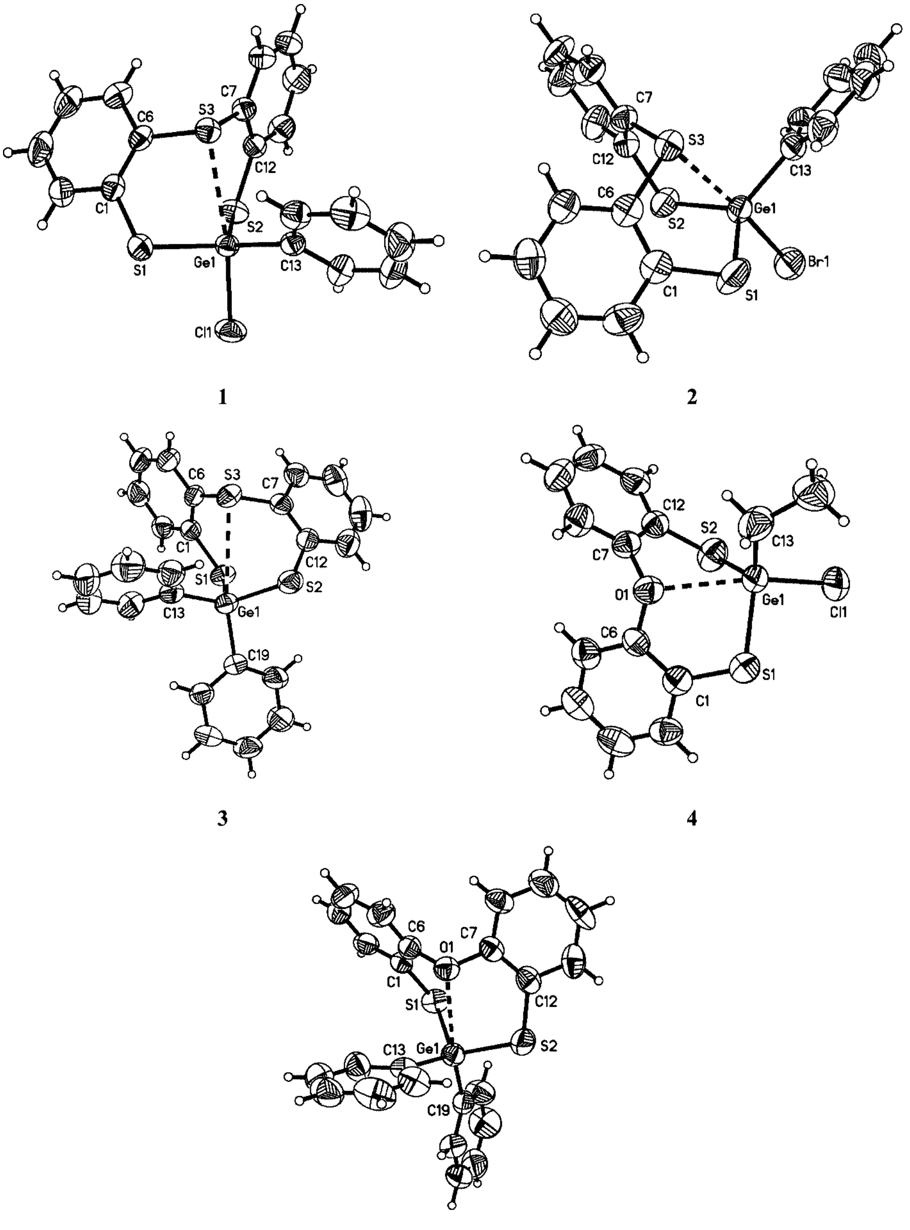

1 **2**

3 **4**

5

Figure 1. ORTEP diagrams of $S(C_6H_4S)_2GePhCl$ (**1**), $S(C_6H_4S)_2GePhBr$ (**2**), $S(C_6H_4S)_2GePh_2$ (**3**), $O(C_6H_4S)_2GeEtCl$ (**4**) and $O(C_6H_4S)_2GePh_2$ (**5**) (50% probability ellipsoids).

given in Table 3. In all compounds, there were no intermolecular interactions between non-hydrogen atoms that were separated by a distance shorter than the sum of their van der Waals radii. This essentially resulted in monomeric molecules.

Table 3. Selected bond lengths [Å] and bond angles [°] of $D(C_6H_4S)_2L_1GeL_2$.

Compound	**1**	**2**	**3**	**4**	**5**
D	S	S	S	O	O
L_1	Cl1	Br1	C19	Cl1	C19
L_2	C13	C13	C13	C13	C13
D→Ge1	2.834(1)	2.782(2)	3.280(1)	2.656(3)	2.872(3)
Ge1–S1	2.236(1)	2.228(2)	2.235(1)	2.231(1)	2.229(1)
Ge1–S2	2.228(1)	2.216(2)	2.255(1)	2.221(1)	2.239(1)
Ge1–L_1	2.233(1)	2.401(1)	1.959(3)	2.187(1)	1.938(4)
Ge1–L_2	1.941(3)	1.943(5)	1.942(4)	1.943(4)	1.954(4)
D→Ge1–L_1	169.57(4)	175.99(4)	168.3(1)	166.97(6)	169.5(1)
S1–Ge1–S2	115.35(4)	114.42(7)	110.58(4)	115.47(5)	111.65(5)
S1–Ge1–L_2	120.5(1)	120.89(2)	112.3(1)	115.0(1)	113.8(1)
S2–Ge1–L_2	119.0(1)	120.2(2)	113.7(1)	116.7(1)	111.6(1)
L_1–Ge1–L_2	101.6(1)	98.6(2)	113.6(1)	108.8(2)	113.4(2)
S1–Ge1–L_1	98.47(4)	97.03(5)	100.6(1)	98.6(1)	100.8(1)
S2–Ge1–L_1	92.46(4)	95.59(5)	105.1(1)	98.86(5)	104.8(1)
C7–D–C6–C1	127.6(3)	125.3(4)	61.0(3)	142.9(3)	87.9(4)
C6–D–C7–C12	–74.4(3)	–77.5(5)	–122.9(3)	–87.4(4)	–137.2(4)
S2–Ge1–S1–C1	–31.1(1)	–40.3(2)	–97.7(1)	–33.0(1)	–94.0(1)
S1–Ge1–S2–C12	99.1(1)	100.7(2)	11.7(1)	98.6(1)	31.9(2)

In all complexes, the Ge–S(thiolate) distances are in good agreement with those reported for eight-membered heterocycles and several other compounds containing germanium–sulfur bonds: 2.191(3) Å in $S(CH_2CH_2S)_2GeCl_2$,[16] 2.154(4)–2.217(4) Å in $O(CH_2CH_2S)_2GeCl_2$,[17] 2.216(1)–2.222(1) and 2.210(3)–2.236(3) Å in the spirocycles $\{O(CH_2CH_2S)_2\}_2Ge$ and $\{S(CH_2CH_2S)_2\}_2Ge$,[18] respectively, 2.111(1)–2.221(1) Å in the homoleptic $Ge(S\text{-}4\text{-}MeC_6H_4)_4$ compound,[19] but significantly shorter than the reported value in the spirocycle $\{PhP(C_6H_4S)_2\}_2Ge$ with a germanium atom in an octahedral local geometry [2.3429(12)–2.4000(10) Å].[11] The Ge–Cl distances in **1** and **4** are 6 and 4% longer, respectively, than that accepted as the common distance for Ge–Cl (2.10 Å in $GeCl_4$)[20] and similar to those found for $D(CH_2CH_2S)_2GeCl_2$ (D = O[17], S[16]); which are longer than that found in the 9,9-dichloro-9-germafluorene [2.1660(9) Å].[21] The Ge–Br distance is 4% longer than that observed for $GeBr_4$ (2.30 Å)[20] and intermediate between those found in $MeN(CH_2CH_2O)_2GeBr_2$ [2.4148(8) and 2.3215(9) Å].[4] The Ge–C distances are in good agreement with other compounds that contain germanium–carbon bonds.[12,22–24]

In addition to the expected bonding of the two sulfur atoms (thiolate-like) and the two exocyclic L_1 and L_2 ligands to germanium, a relatively short distance involving the transannular D and Ge atoms is observed (D = S in **1**, **2** and **3**; D = O in **4** and **5**). The S→Ge bond lengths in **1**, **2** and **3** are 2.834(1), 2.782(2) and 3.280(1) Å, respectively, which are 27, 24 and 46% longer than the covalent radii sum of Ge and S (2.24 Å)[25] but significantly shorter than the van der Waals radii sum (3.75 Å).[1,14] The magnitude of these distances is consistent with the existence of a secondary bonding.[1] These S→Ge distances in **1**, **2** and **3** are similar for the spirocycles $S(CH_2CH_2S)_2GeSO(C_2H_4)$ [2.842(1) Å],[2] $[S(CH_2CH_2S)_2]_2Ge$ [3.237(3) and 3.453(3) Å],[18] and $S(CH_2CH_2S)_2GeCl_2$ [3.01(3) Å],[16] and significantly longer than that reported for the spirocycle $[S(C_6H_4O)_2]_2Ge$ [2.447(1) Å].[14]

The O→Ge distances in **4** [2.656(3) Å] and **5** [2.872(3) Å] are significantly shorter than the van der Waals radii sum of Ge and O (3.47 Å)[1] and 41% and 53% longer than the covalent radii sum (1.88 Å),[2,25] respectively. The observed O→Ge bond lengths in **4** and **5** are significantly longer than those reported for $O(CH_2CH_2S)_2GeCl_2$ [2.36(1) and 2.39(1) Å],[17] for the spirocycles containing pentacoordinate germanium $O(CH_2CH_2S)_2GeSO(C_2H_4)$ [2.492(3) Å] and $O(CH_2CH_2S)_2GeS_2(C_2H_4)$ [2.616(1) Å], and shorter than those reported for the spiro compound containing hexacoordinate germanium $[O(CH_2CH_2S)_2]_2Ge$ displaying two crystallographic independent molecules in the solid state [2.914(3), 3.040(3), 2.955(3) and 2.946(3) Å][18]. If the transannular interaction (D→Ge) is taken into account, the geometry of the coordination sphere of the germanium atom can be described as trigonal bipyramidal (TBP), where the halogen (for **1**, **2** and **4**), carbon (for **3** and **5**) and D donor atoms (S for **1**, **2**, **3**, O for **4**, **5**) are in the axial positions, meanwhile the two thiolate-like sulfur and carbon atoms occupy equatorial positions.

Following the Holmes procedure based on the donor-acceptor atom bond length,[26–28] the degree of displacement at the Ge atom from tetrahedral to trigonal-bipyramidal geometry (TBP) was determined. Additionally and in order to evaluate the magnitude of the interaction based

Table 4. Comparison of D→Ge–L_1 geometrical bond parameters in complexes **1**–**5**; bond lengths [Å], bond angles [°], % TBP and Pauling bond order.

Compound	D	L_1	L_2	D→Ge	D→Ge–L1	% TBP	Δd[a]	BO[b] D→Ge
1	S	Cl	Ph	2.834(1)	169.57(4)	60.7	0.594	0.1453
2	S	Br	Ph	2.782(2)	175.99(4)	64.1	0.542	0.1721
3	S	Ph	Ph	3.280(1)	168.3(1)	31.1	1.038	0.0343
4	O	Cl	Et	2.656(3)	166.97(6)	51.2	0.778	0.0799
5	O	Ph	Ph	2.872(3)	169.5(1)	37.6	0.992	0.0399

[a] Bond widening, $\Delta d = (d_{\text{exp}} - \Sigma r_{\text{cov}})$, according to standard bond lengths d(Ge S) 2.24, d(Ge O) 1.88.[1,2,14,25] [b] Mode of calculation BO = $10^{-(1.41 \cdot \Delta d)}$.[29,30]

on the distances, the Pauling-type bond order, BO, for the transannular interactions (D→Ge) in all compounds was also calculated.[29,30]These results are reported in Table 4.

The TBP% for halogen compounds are larger than those for other compounds in the series, indicating the importance of attaching an electronegative ligand to germanium in order to expand its coordination number.

In all compounds the eight-membered ring conformation can be described as a twist boat (C_1 symmetry) according to the torsion angle data, where the double phenylated **3** and **5** compounds are most distorted when the TBP and BO order are smaller.

Theoretical Study

In order to study the intramolecular interactions (D→Ge) we carried out theoretical calculations. Hence, each one of the compounds **1**–**5** was modelled with a GaussView visualizer,[31] followed by a geometry optimisation with the PM3 semi-empirical method[32]. A further geometry optimisation was carried out with density functional theory (DFT) using the hybrid B3LYP functional[33]. For our DFT computations we employed the relativistic Stuttgart-Dresden Effective Core Potential for Ge[34] along with its Triple-Zeta correlation consistent basis set[35]. For all the other atoms in compounds **1** to **5**, Dunning's Double-Zeta correlation consistent all electron basis set[36] was used. The basis sets we employed include polarisation and diffusion functions. Hereafter these calculations will be referred to as B3LYP ccSDDTZ. The computed bond orders, interatomic overlaps and charges reported herein were computed within the NBO approach.[37] All our calculations were carried out with the suite of programmes in Gaussian 03.[38]

Theoretical Results and Discussion

All optimised molecular conformations for **1**–**5** are in good agreement when compared with those observed by X-ray crystallographic data. A selected set of bond lengths and bond and torsion angles is listed in Table 5. It is relevant to mention that we explored the two possible geometrical isomers for complexes **1**, **2** and **4**, i.e. those with the halogen ligand in an axial or in an equatorial position, where isomers that resemble the conformation determined by X-ray diffraction experiments were the most stable. These correspond to the lowest energy conformation of those obtained with the procedure previously outlined. A comparison between the X-ray and the computed D–Ge bond lengths shows a remarkable difference for compounds **1**, **2** and **3**. The largest difference is for compound **2** (≈0.39 Å), followed by that of compounds **1** and **3**, ≈0.32 Å and ≈0.05 Å respectively, whereas for compounds **4** and **5** we noticed that the distances O→Ge are ca. 0.13 Å and 0.07 Å larger than those obtained by X-ray spectroscopy at 298 K. The DFT calculations at the level employed reproduce well the experimental overall geometries; the observed differences in the geometrical parameters are not unusual[3] and may be due to the temperature of the diffraction experiments as well as the packing forces in the crystal.

NBO Analysis

In Table 6 the computed Wiberg bond index values for a selected number of atoms in compounds **1**–**5** are reported. It is worth noting that this index has approximately the same value for all germanium–sulfur thiolate bonds. However, in **1**–**3** this bond index is bigger for the S(thiolate-

Table 5. Selected bond lengths [Å] and angles [°] for compounds **1**–**5**. **a** columns are data from X-ray characterisation. **b** columns are data obtained from B3LYP ccSDDTZ computations.

Compound	**1a**	**1b**	**2a**	**2b**	**3a**	**3b**	**4a**	**4b**	**5a**	**5b**
D	S	S	S	S	S	S	O	O	O	O
L1	Cl1	Cl1	Br1	Br1	C19	C19	Cl1	Cl1	C19	C19
L2	C13	C13	C13	C13	C13	C13	C13	C13	C13	C13
D→Ge1	2.834(1)	3.157	2.782(2)	3.181	3.280(1)	3.328	2.656(3)	2.781	2.872(3)	2.944
Ge1–S1	2.236(1)	2.278	2.228(2)	2.280	2.235(1)	2.281	2.231(1)	2.272	2.229(1)	2.286
Ge1–S2	2.228(1)	2.273	2.216(2)	2.273	2.255(1)	2.297	2.221(1)	2.278	2.239(1)	2.288
Ge1–L1	2.233(1)	2.215	2.401(1)	2.377	1.959(3)	1.970	2.187(1)	2.210	1.938(4)	1.966
Ge1–L2	1.941(3)	1.953	1.943(5)	1.955	1.942(4)	1.960	1.943(4)	1.969	1.954(4)	1.960
D→Ge1–L1	169.57(4)	169.79	175.99(4)	169.69	168.3(1)	170.32	166.97(6)	169.89	169.5(1)	168.40
D→Ge1–S1	77.60(3)	72.68	80.64(5)	72.14	73.36(3)	73.71	74.35(6)	72.75	71.94(6)	70.80
D→Ge1–S2	80.76(3)	76.42	82.45(5)	76.01	68.78(3)	69.61	75.17(6)	73.40	71.98(6)	69.56
D→Ge1–L2	88.7(1)	84.90	85.3(2)	84.40	78.2(1)	78.66	84.2(1)	84.16	76.8(1)	79.05
S1–Ge1–L1	98.47(4)	102.75	97.03(5)	103.09	100.6(1)	102.79	98.57(5)	102.08	100.8(1)	104.43
S2–Ge1–L1	92.46(4)	97.84	95.59(5)	98.27	105.1(1)	104.07	98.86(5)	101.84	104.8(1)	103.83
S1–Ge1–S2	115.35(4)	114.14	114.42(7)	113.96	110.58(4)	111.01	115.47(5)	114.93	111.65(5)	112.52
S1–Ge1–L2	120.5(1)	115.14	120.9(2)	114.68	112.4(1)	113.63	115.0(1)	113.92	113.8(1)	110.83
S2–Ge1–L2	119.0(1)	118.13	120.2(2)	117.81	113.7(1)	113.49	116.7(1)	115.79	111.6(1)	112.28
L1–Ge1– L2	101.6(1)	105.30	98.6(2)	105.91	113. 6(1)	110.90	108.8(2)	105.94	113.4(2)	112.52
C6–D–C7	101.7(2)	103.58	101.7(3)	103.56	103.0(2)	103.57	116.6(3)	118.33	116.3(3)	118.28
S2–Ge1–S1–C1	–31.1(1)	–19.40	–40.3(2)	–18.33	–97.7(1)	–95.25	–33.0(1)	–29.68	–94.0(1)	–91.76
S1–Ge1–S2–C12	99.1(1)	97.02	100.7(2)	96.56	11.7(1)	15.49	98.6(1)	95.50	31.9(2)	23.31

like)→Ge than for the S(thioether-like)→Ge interaction. A similar trend is exhibited by the O→Ge interaction in compounds **4** and **5**.

Table 6. NBO values of Wiberg bond index for a selected number of atoms in compounds **1**–**5**. Data from B3LYP ccSDDTZ computations.

Compound	**1**	**2**	**3**	**4**	**5**
D	S	S	S	O1	O1
L1	Cl1	Br1	C19	Cl1	C19
L2	C13	C13	C13	C13	C13
D→Ge1	0.1080	0.1027	0.0594	0.0579	0.0357
Ge1–S1	0.8308	0.8303	0.8561	0.8438	0.8478
Ge1–S2	0.8506	0.8543	0.8185	0.8349	0.8350
Ge1–L1	0.7757	0.8356	0.7233	0.7880	0.7326
Ge1–L2	0.7154	0.7149	0.7260	0.7538	0.7292
D–C6	1.0088	1.0091	1.0258	0.9120	0.9089
D–C7	1.0201	1.0207	1.0121	0.9012	0.9245
S1–C1	1.0557	1.0551	1.0628	1.0587	1.0587
S2–C12	1.0634	1.0611	1.0558	1.0587	1.0565

To study the nature of this short Wiberg bond index, the computed overlap-weighted natural atomic orbital values are reported in Table 7. From this table it is possible to observe that compounds **1**–**3**, which contain the S→Ge interaction, have larger overlap values than compounds **4** and **5**, which contain the O→Ge interaction. It is important to observe that **3** and **5** exhibit the smallest overlap value in these two groups of molecules.

Table 7. NBO computed overlap-weighted natural atomic orbital values for compounds **1**–**5**. Data from computations with B3LYP cc-SDDTZ basis sets.

Compound	**1**	**2**	**3**	**4**	**5**
D	S3	S3	S3	O1	O1
L1	Cl1	Br1	C19	Cl1	C19
L2	C13	C13	C13	C13	C13
D→Ge1	0.1484	0.1429	0.0906	0.0877	0.0559
Ge1–S1	0.7770	0.7728	0.7757	0.7880	0.7685
Ge1–S2	0.7899	0.7885	0.7516	0.7810	0.7632
Ge1–L1	0.7314	0.7899	0.7318	0.7389	0.7410
Ge1–L2	0.7403	0.7336	0.7406	0.7614	0.7438

As a final element for our theoretical analysis we report, in Table 8, the charges obtained within the NBO procedure. It may be observed that the sulfur donor atoms in compounds **1**–**3** exhibit approximately the same positive charge, whereas the thiolate-like sulfur atoms roughly have the same negative charge. This may be a consequence of the different environments of the sulfur atoms in the dibenzotrithiagermocines: atoms S1 and S2 are dicoordinate and covalently bonded to a rather electropositive germanium atom while the S3 atom is bonded to a more electronegative carbon atom and also shares its electron density with the acidic germanium(IV) atom. The O1 atom in **4** and **5** has the same negative charge, according to the electronegativity of oxygen.

Table 8. Selected atom charges obtained within the NBO procedure for compounds **1**–**5**. Computations with B3LYP cc-SDDTZ basis sets.

Compound	**1**	**2**	**3**	**4**	**5**
D	S3	S3	S3	O1	O1
D	0.30	0.30	0.30	–0.56	–0.56
S1	–0.13	–0.13	–0.13	–0.12	–0.13
S2	–0.11	–0.11	–0.16	–0.11	–0.15
Ge3	1.28	1.19	1.40	1.29	1.40
Cl1	–0.41	–	–	–0.41	–
Br1	–	–0.32	–	–	–
C13	–0.51	–0.51	–0.50	–0.89	–0.50
C19	–	–	–0.50	–	–0.50

Discussion

The calculated Wiberg bond index values in Table 6 show the existence of a bond interaction between the D→Ge (where D = S or O) in compounds **1** to **5**. The reported numerical values in Table 7 for the NAO overlap-weighted analysis confirm this bond possibility and give it a covalent like character. However, the reported atomic charges in Table 8 suggest the possibility of interatomic interactions with a Coulombic character.

We may conclude that the interaction S3→Ge in **1** and **2** has two components: one covalent and a second one with a Coulombic character. In these two compounds the interaction is dominated by a covalent interaction, which screens the positive–positive S3–Ge Coulomb interaction. This behaviour is enhanced by the halogen atom coordinated to Ge and its role in the Coulomb field within the molecule. Similar arguments may be given to the O1→Ge interaction in **4**. However, in this case, the negative charge on the oxygen donor atom increases the intensity of the Coulomb field making this the dominant part of this interaction.

In compounds **3** and **5** we have the opportunity to appreciate how this covalent-Coulombic dual character works. In this case we do not have halogen atoms to enhance the interchange. Hence S3→Ge in **3** has a more covalent than Coulombic character, whereas O1→Ge is dominated by a strong Coulomb interaction, which makes their intramolecular distances shorter supporting the results of the structural analyses in terms of our TBP and BO analyses for these complexes.

Conclusions

In order to study the phenomena of hypercoordination in germanium heterocyclic compounds we have synthesised and fully structurally characterised five new dibenzogermocines **1**–**5** by employing tridentate $[D(C_6H_4S)_2]^{2-}$ ligands. All compounds exhibit a bipyramidal-trigonal local geometry of the germanium(IV) atom with intramolecular interactions D→Ge. Geometry optimisations at the DFT level of theory, using the hybrid functional B3LYP renders molecular conformations in good agreement to those determined by X-ray diffraction studies. An NBO analysis was carried out on this electron structure. The TBP and BO analysis for the crystalline molecular structure and our NBO analysis show similar behaviour for the D→Ge interaction, which is enhanced by the presence of the halogen ligands.

Experimental Section

General Procedures: All manipulations were performed under a dry, oxygen-free argon atmosphere using standard Schlenk techniques. Solvents were dried by standard methods and distilled prior to use. Melting points were determined with a Melt-Temp II instrument and are uncorrected. Spectra were recorded with the following instruments. Mass spectra: FAB-mass spectra were recorded with a JEOL JMS-AX505HA by using a Xe beam at 6 keV, with nitrobenzyl alcohol (NBA) as matrix. For EI, a Hewlett Packard 5989A mass spectrometer was used. Elemental analyses: Perkin–Elmer Series II CHNS/O Analyser. The IR spectra were record in the 4000-400 cm^{-1} range with a Perkin–Elmer System 2000 FT-IR spectrometer, as KBr pellets. NMR: Jeol Eclipse 400 spectrometer; with the residual protio-solvent signal used as referenced for ^{1}H NMR spectra. ^{13}C{^{1}H} NMR spectra were referred through the solvent peaks. Chemical shifts are quoted on the δ scale (downfield shifts are positive) relative to tetramethylsilane (^{1}H, ^{13}C{^{1}H} NMR spectra). Spectra were recorded at 25 °C. ^{1}H NMR spectra; 399.78 MHz, ^{13}C{^{1}H} NMR spectra; 100.53 MHz. $S(C_6H_4SH)_2$[15] and $O(C_6H_4SH)_2$[9] were synthesised according to literature methods. $PhGeCl_3$, Ph_2GeCl_2, $EtGeCl_3$, *n*BuLi (1.6 M, in hexanes), KBr and HBr were purchased from Aldrich and Fluka and were used as supplied.

$S(C_6H_4S)_2GePhCl$ (1): *n*BuLi in hexanes (1.6 M, 5.5 mL, 8.8 mmol) was added to a solution containing $S(C_6H_4SH)_2$ (1.0 g, 4.0 mmol) in THF (40 mL) at 0 °C. After the solution was stirred for 30 min, a red solution resulted, $PhGeCl_3$ (0.66 mL, 4.0 mmol) was added via a syringe. The solution was kept overnight at room temperature. The colourless solution was refluxed for 4 h, and then the resultant heterogeneous reaction mixture was cooled to room temperature. The precipitate of LiCl was removed by filtration. Volatiles were removed under an argon flow to provide colourless crystals of **1**, which were washed with hexanes (40 mL) and filtered by suction. Yield: 1.50 g (86%). Mass spectrum (FAB+) *m*/*z* (rel int) = 434 (5) [M$^+$], 399 (50) [M$^+$ – Cl], 216 (45) [M$^+$ – Cl–PhSGe]. M.p. 201–203 °C. $S(C_6H_5S)_2GePhCl$: calcd. C 49.56, H 3.22; found C 49.76, H 3.20. ^{1}H NMR (CDCl$_3$): δ = 7.16 (ddd, $^3J_{3\text{-H},2\text{-H}} = {}^3J_{3\text{-H},4\text{-H}}$ = 7.74, $^4J_{3\text{-H},1\text{-H}}$ = 1.44 Hz, 2 H, 3-H), 7.27 (ddd, $^3J_{2\text{-H},1\text{-H}} = {}^3J_{2\text{-H},3\text{-H}}$ = 7.74, $^4J_{2\text{-H},4\text{-H}}$ = 1.44 Hz, 2 H, 2-H), 7.40 (m, 3 H, 6-H and 7-H), 7.44 (dd, $^3J_{4\text{-H},3\text{-H}}$ = 7.74, $^4J_{4\text{-H},2\text{-H}}$ = 1.44 Hz, 2 H, 4-H), 7.65 (dd, $^3J_{1\text{-H},2\text{-H}}$ = 7.74, $^4J_{1\text{-H},3\text{-H}}$ = 1.44 Hz, 2 H, 1-H), 7.81 (m, 2 H, 5-H) ppm. ^{13}C{^{1}H} NMR (CDCl$_3$): δ = 127.5, 128.9, 129.9, 130.9, 131.1, 131.2, 132.2, 134.2, 140.7, 141.5 ppm. IR (KBr pellet): ṽ = 3045, 1568, 1480, 1445, 1430, 1247, 1078, 1040, 1032, 851, 754, 733, 714, 689, 657 cm^{-1}.

$S(C_6H_4S)_2GePhBr$ (2): $S(C_6H_4S)_2GePhCl$ (**1**, 0.26 g, 0.60 mmol), KBr (0.18 g, 1.5 mmol) and HBr 48% (2 mL) were suspended in benzene (25 mL) and refluxed for 16 h. The water was removed from the resulting colourless solution by means of a Dean–Stark trap. The solution obtained was dried by means of a column of Celite and Na_2SO_4. The solution was left under an argon flow to provide colourless crystals of **2**, which were washed with hexanes (40 mL) and filtered by suction. Yield: 180 mg (63%). Mass spectrum (FAB+) *m*/*z* (rel int) = 478 (3) [M$^+$], 399 (50) [M$^+$ – Cl], 216 (20) [M$^+$ – Cl – PhSGe]. M.p. 197–199 °C. $S(C_6H_5S)_2GePhBr$: calcd. C 45.23, H 2.74; found C 45.96, H 2.74. ^{1}H NMR (CDCl$_3$): δ = 7.16 (ddd, $^3J_{3\text{-H},2\text{-H}} = {}^3J_{3\text{-H},4\text{-H}}$ = 7.68, $^4J_{3\text{-H},1\text{-H}}$ = 1.48 Hz, 2 H, 3-H), 7.27 (ddd, $^3J_{2\text{-H},1\text{-H}} = {}^3J_{2\text{-H},3\text{-H}}$ = 7.68, $^4J_{2\text{-H},4\text{-H}}$ = 1.48 Hz, 2 H, 2-H), 7.39 (m, 3 H, 6-H and 7-H), 7.44 (dd, $^3J_{4\text{-H},3\text{-H}}$ = 7.68, $^4J_{4\text{-H},2\text{-H}}$ = 1.48 Hz, 2 H, 4-H), 7.65 (dd, $^3J_{1\text{-H},2\text{-H}}$ = 7.68, $^4J_{1\text{-H},3\text{-H}}$ = 1.48 Hz, 2 H, 1-H), 7.78 (m, 2 H, 5-H) ppm. ^{13}C{^{1}H} NMR (CDCl$_3$): δ = 127.5, 128.9, 129.9, 130.9, 131.0, 132.1, 132.3, 134.3, 140.7,141.9 ppm. IR (KBr pellet): ṽ = 3050, 1568, 1445, 1442, 1249, 1081, 1039, 862, 735, 730, 710, 692 cm^{-1}.

$S(C_6H_5S)_2GePh_2$ (3): This compound was prepared in a similar fashion to compound **1**, with $S(C_6H_4SH)_2$ (0.42 g, 1.68 mmol), *n*BuLi in hexanes (1.6 M, 2.3 mL, 3.7 mmol) and Ph_2GeCl_2 (0.35 mL, 1.68 mmol). Colourless crystals were obtained. Yield: 0.50 g (63%). Mass spectrum (FAB+) *m*/*z* (rel int) = 476 (18) [M$^+$], 399 (base peak) [M$^+$ – Ph], 216 (65) [M$^+$ – Ph – Ph – SGe]. M.p. 126–128 °C. $S(C_6H_5S)_2Ph_2Ge$: calcd. C 60.66, H 3.82; found C 60.83, H 3.98. ^{1}H NMR (CDCl$_3$): δ = 7.13 (ddd, $^3J_{2\text{-H},1\text{-H}} = {}^3J_{2\text{-H},3\text{-H}}$ = 7.72, $^4J_{2\text{-H},4\text{-H}}$ = 1.44 Hz, 2 H, 2-H), 7.18 (ddd, $^3J_{3\text{-H},2\text{-H}} = {}^3J_{3\text{-H},4\text{-H}}$ = 7.72, $^4J_{3\text{-H},1\text{-H}}$ = 1.44 Hz, 2 H, 3-H), 7.34 (m, 6 H, 6-H and 7-H), 7.44 (dd, $^3J_{4\text{-H},3\text{-H}}$ = 7.72, $^4J_{4\text{-H},2\text{-H}}$ = 1.44 Hz, 2 H, 4-H), 7.63 (m, 4 H, 5-H), 7.66 (dd, $^3J_{1\text{-H},2\text{-H}}$ = 7.72, $^4J_{1\text{-H},3\text{-H}}$ = 1.44 Hz, 2 H, 1-H) ppm. ^{13}C{^{1}H} NMR (CDCl$_3$): δ = 127.4, 128.4, 128.5, 130.0, 133.2, 134.3, 134.9, 137.4, 138.2, 139.8 ppm. IR (KBr pellet): 3066, 3047, 1568, 1480, 1444, 1431, 1248, 1085, 1040, 859, 752, 734, 716, 693 cm^{-1}.

$O(C_6H_4S)_2GeEtCl$ (4): This compound was prepared in a similar fashion to compound **1**, with $O(C_6H_4SH)_2$ (0.92 g, 3.9 mmol), *n*BuLi in hexanes (1.6 M, 5.0 mL, 8.0 mmol) and $EtGeCl_3$ (0.5 mL, 3.9 mmol). The solid was filtered and recrystallised from *i*-PrOH. Colourless crystals were obtained. Yield: 0.20 g (28%). Mass spectrum (EI-MS, CHCl$_3$, 30 eV) *m*/*z* (rel int) = 370 (10) [M$^+$], 341 (20) [M$^+$ – Et], 305 (10) [M$^+$ – Et – Cl], 200 (base peak) [M$^+$ – Et–Cl–GeS]. M.p. 96–98 °C. $O(C_6H_4S)_2EtGeCl$: calcd. C 45.51, H 3.55; found C 45.80, H 3.55. ^{1}H NMR (CDCl$_3$): δ = 1.18 (t, $^3J_{6\text{-H},5\text{-H}}$ = 7.70 Hz, 3 H, 6-H), 1.80 (q, $^3J_{5\text{-H},6\text{-H}}$ = 7.70 Hz, 2 H, 5-H), 7.13 (dd, $^3J_{4\text{-H},3\text{-H}}$ = 7.70, $^4J_{4\text{-H},2\text{-H}}$ = 1.48 Hz, 2 H, 4-H), 7.15 (ddd, $^3J_{2\text{-H},1\text{-H}} = {}^3J_{2\text{-H},3\text{-H}}$ = 7.70, $^4J_{2\text{-H},4\text{-H}}$ = 1.48 Hz, 2 H, 2-H), 7.23 (ddd, $^3J_{3\text{-H},2\text{-H}} = {}^3J_{3\text{-H},4\text{-H}}$ = 7.70, $^4J_{3\text{-H},1\text{-H}}$ = 1.48 Hz, 2 H, 3-H), 7.53 (dd, $^3J_{1\text{-H},2\text{-H}}$ = 7.70, $^4J_{1\text{-H},3\text{-H}}$ = 1.48 Hz, 2 H, 1-H) ppm. ^{13}C{^{1}H} NMR (CDCl$_3$): δ = 8.3, 23.0, 120.2, 125.8, 126.2, 132.6, 152.7 ppm. IR (KBr pellet): 3061, 2958, 2923, 2868, 1564, 1462, 1440, 1210, 1061, 869, 799, 757, 732, 700 cm^{-1}.

$O(C_6H_5S)_2GePh_2$ (5): This compound was prepared in a similar fashion to compound **1**, with $O(C_6H_4SH)_2$ (0.39 g, 1.66 mmol), *n*BuLi in hexanes (1.6 M, 2.3 mL, 3.7 mmol) and Ph_2GeCl_2 (0.35 mL, 1.68 mmol). Colourless crystals were obtained. Yield: 0.20 g (26%). Mass spectrum (FAB+) *m*/*z* (rel int) = 460 (35) [M$^+$], 383 (base peak) [M$^+$ – Ph], 200 (95) [M$^+$ – Ph – PhGeS]. M.p. 105–107 °C. $O(C_6H_5S)_2Ph_2Ge$: calcd. C 62.78, H 3.95; found C 63.04, H 3.97. ^{1}H NMR (CDCl$_3$): δ = 6.85 (dd, $^3J_{4\text{-H},3\text{-H}}$ = 7.36, $^4J_{4\text{-H},2\text{-H}}$ = 1.80 Hz, 2 H, 4-H), 7.04 (ddd $^3J_{3\text{-H},2\text{-H}} = {}^3J_{3\text{-H},4\text{-H}}$ = 7.36, $^4J_{3\text{-H},1\text{-H}}$ = 1.80 Hz, 2 H, 3-H), 7.09 (ddd, $^3J_{2\text{-H},1\text{-H}} = {}^3J_{2\text{-H},3\text{-H}}$ = 7.36, $^4J_{2\text{-H},4\text{-H}}$ = 1.80 Hz, 2 H, 2-H), 7.32 (m, 6 H, 6-H and 7-H), 7.56 (dd, $^3J_{1\text{-H},2\text{-H}}$ = 7.36, $^4J_{1\text{-H},3\text{-H}}$ = 1.80 Hz, 2 H, 1-H), 7.65 (m, 4 H, 5-H^5) ppm. ^{13}C{^{1}H} NMR (CDCl$_3$): δ = 120.6, 124.7, 126.6, 127.5, 128.4, 130.1, 133.6, 133.7, 136.4, 154.8 ppm. IR (KBr pellet): 3047, 3011, 1565, 1462, 1430, 1249, 1214, 1089, 1063, 870, 800, 763, 755, 733, 696, 669 cm^{-1}.

X-ray Crystallography: Suitable single crystals of the complexes **1**, **2**, **3** and **5** were grown by slow evaporation from a chloroform solution. Compound **4** was crystallised from *i*-PrOH. X-ray diffraction data on **1**–**5** were collected at room temperature on a CCD Smart 6000 diffractometer through the use of Mo-K_α radiation (λ = 0.71073 Å, graphite monochromator). Data were integrated,

Table 9. Selected crystallographic data for compounds **1**–**5**.

Compound	**1**	**2**	**3**	**4**	**5**
Empirical formula	$C_{18}H_{13}ClGeS_3$	$C_{18}H_{13}BrGeS_3$	$C_{24}H_{18}GeS_3$	$C_{14}H_{13}ClGeOS_2$	$C_{24}H_{18}GeOS_2$
M_r [g·mol^{-1}]	433.50	477.96	475.15	369.40	459.09
Crystal size [mm]	0.6 × 0.2 × 0.1	0.6 × 0.13 × 0.08	0.5 × 0.3 × 0.13	0.12 × 0.26 × 0.60	0.17 × 0.23 × 0.48
Crystal system	monoclinic	triclinic	monoclinic	monoclinic	triclinic
Space group	$P21/c$	$P\bar{1}$	$P21/n$	$P21/n$	$P\bar{1}$
ρ_{calc} [Mg·m^{-3}]	1.592	1.712	1.440	1.593	1.441
Z	4	2	4	4	2
a [Å]	9.7904(6)	8.9753(9)	10.8082(9)	10.0723(9)	9.3682(8)
b [Å]	10.2618(7)	9.836(1)	14.626(1)	11.301(1)	9.3892(8)
c [Å]	18.296(1)	12.083(1)	13.961(1)	13.850(1)	12.376(1)
α [°]	90	79.655(2)	90	90	85.188(2)
β [°]	100.305(2)	72.417(3)	96.755(2)	102.297(2)	83.538(2)
γ [°]	90	66.041(2)	90	90	78.649(2)
V [Å^3]	1808.5(2)	927.3(2)	2191.6(3)	1540.3(2)	1058.4(2)
μ [mm^{-1}]	2.183	4.139	1.691	2.421	1.656
F(000)	872	472	968	744	468
GoF	0.909	0.963	0.811	0.837	0.930
Abs. correction	SADABS	SADABS	SADABS	SADABS	SADABS
Reflections collected	11696	6117	14261	10798	7098
Unique reflections R_{int}	3540; 0.0467	3624; 0.0304	4296; 0.0568	3362; 0.0480	4167; 0.0289
R_1, wR_2 [$I > 2\sigma(I)$]	0.0357, 0.0794	0.0440, 0.1144	0.0399, 0.0771	0.0426, 0.0892	0.0450, 0.0960
R_1, wR_2 (all data)	0.0566, 0.0851	0.0785, 0.1249	0.0800, 0.0859	0.0842, 0.0991	0.0770, 0.1168
Large residuals [e·Å^{-3}]	0.715/–0.427	0.592/–0.790	0.496/–0.268	0.646/–0.322	0.524/–0.260

scaled, sorted and averaged using the SMART software package. The structures were solved by direct methods, using SHELXTL NT Version 5.10 and refined by full-matrix least-squares against F^2.[39] An empirical absorption correction based on the multiple measurement of equivalent reflections was applied by using the programme SADABS.[40] The displacement parameters of non-hydrogen atoms were refined anisotropically. The positions of the hydrogen atoms were kept fixed with a common isotropic displacement parameter. Selected crystallographic data are given in Table 9.[41]

Acknowledgments

J. A. C. wants to thank David Vazquez for the running of the computers and network at IQ-UNAM. We acknowledge DGSCA-UNAM for the generous allocation of CPU time. S. G. M. fully acknowledges the scholarship from CONACyT. This research was supported by CONACyT (Project 44009).

---

[1] N. W. Alcock, *Adv. Inorg. Chem. Radiochem.* **1972**, *15*, 1–58.

[2] R. Cea Olivares, V. García Montalvo, M. M. Moya Cabrera, *Coord. Chem. Rev.* **2005**, *249*, 859–872, and references cited therein.

[3] S. S. Karlov, E. K. Lermontova, M. V. Zabalov, A. A. Selina, A. V. Churakov, J. A. K. Howard, M. Yu. Antipin, G. S. Zaitseva, *Inorg. Chem.* **2005**, *44*, 4879–4886.

[4] S. S. Karlov, E. Kh. Yajuboca, E. V. Gauchenova, A. A. Selina, A. V. Churakov, J. A. K. Howard, D. A. Tyurin, J. Lorberth, G. S. Zaitseva, *Z. Naturforsch., Teil B* **2003**, *58*, 1165–1170.

[5] M. Beuter, U. Kolb, A. Zickgraf, E. Braeu, M. Bletz, M. Draeger, *Polyhedron* **1997**, *16*, 4005–4015.

[6] E. Braeu, A. Zickgraf, M. Draeger, E. Mocellin, M. Maeda, M. Takahashi, M. Takeda, C. Mealli, *Polyhedron* **1998**, *17*, 2655–2668.

[7] K. Jurkschat, J. Schilling, C. Mugge, A. Tzschach, J. Meunier Piret, M. van Meerssche, M. Gielen, R. Willem, *Organometallics* **1988**, *7*, 38–46.

[8] A. Zschunke, A. Tzschach, K. Jurkschat, *J. Organomet. Chem.* **1976**, *112*, 273–278.

[9] References cited in J. G. Alvarado Rodríguez, N. Andrade López, S. González Montiel, G. Merino, A. Vela, *Eur. J. Inorg. Chem.* **2003**, 3554–3561.

[10] J. G. Alvarado Rodríguez, N. Andrade López, S. González Montiel, *Eur. J. Inorg. Chem.* in press.

[11] M. Y. Chiang, L. Jing Wei, W. Feng Zeng, *Acta Crystallogr., Sect. C* **2005**, *61*, m84–m85.

[12] T. Thompson, S. D. Pastor, G. Rihs, *Inorg. Chem.* **1999**, *38*, 4163–4167.

[13] D. Pastor, V. Huang, D. NabiRahni, *Phosphorus, Sulfur Silicon Relat. Elem.* **1998**, *139*, 87–96.

[14] D. Pastor, V. Huang, D. NabiRhani, *Inorg. Chem.* **1997**, *36*, 5966–5968.

[15] D. Sellmann, D. Haussinger, *Eur. J. Inorg. Chem.* **1999**, 1715–1725.

[16] M. Draeger, *Chem. Ber.* **1975**, *108*, 1723–1730.

[17] M. Draeger, *Z. Anorg. Allg. Chem.* **1976**, *423*, 53–66.

[18] C. Deng Hai, C. Hung Cheh, U. Chuen Her, *Inorg. Chim. Acta* **1993**, *208*, 99–101.

[19] B. Kersting, B. Krebs, *Inorg. Chem.* **1994**, *33*, 3886–3892.

[20] J. E. Huheey, E. A. Keiter, R. L. Keiter, *Inorganic Chemistry: Principles of Structure and Reactivity*, 4th ed., Harper Collins College Publishers, New York, NY, **1993**, A30.

[21] Y. Liu, D. Ballweg, T. Müller, I. A. Guzei, R. W. Clark, R. West, *J. Am. Chem. Soc.* **2002**, *124*, 12174–12181.

[22] S. D. Pastor, A. R. Smith, G. Rihs, *Phosphorus Sulfur Silicon Relat. Elem.* **1996**, *115*, 169–177.

[23] K. Tani, S. Kato, T. Kanda, S. Inagaki, *Org. Lett.* **2001**, *3*, 655–657.

[24] A. K. Brisdon, I. R. Crossley, R. G. Pritchard, J. E. Warren, *Inorg. Chem.* **2002**, *41*, 4748–4755.

[25] W. W Porterfield, *Inorganic Chemistry: A Unified Approach*, 2nd ed., Academic Press, San Diego, Cal, **1993**, p. 214.

[26] A. Chandrasekaran, P. Sood, R. O. Day, R. R. Holmes, *Inorg. Chem.* **1999**, *38*, 3369–3376.

[27] N. V. Timosheva, A. Chandrasekaran, R. O. Day, R. R. Holmes, *Inorg. Chem.* **1998**, *37*, 3862–3867.

[28] D. J. Sherlock, A. Chandrasekaran, R. O. Day, R. R. Holmes, *Inorg. Chem.* **1997**, *36*, 5082–5089.

[29] L. Pauling, *The Nature of the Chemical Bond*, 3rd ed., Cornell University Press, Ithaca, NY, **1960**, p. 239.

[30] U. Kolb, M. Beuter, M. Gerner, M. Draeger, *Organometallics* **1994**, *13*, 4413–4425.
[31] *Gauss View Version 2.06*, Gaussian, Inc. Pittsburgh PA, USA.
[32] J. J. P. Stewart, *J. Comput. Chem.* **1989**, *10*, 209-220; J. J. P. Stewart, *J. Comput. Chem.* **1989**, *10*, 221–264.
[33] A. D. Becke, *J. Chem. Phys.* **1993**, *98*, 5648–5652.
[34] A. Bergner, M. Dolg, W. Kuechle, H. Stoll, H. Preuss, *Mol. Phys.* **1993**, *80*, 1431–1441.
[35] J. M. L. Martin, A. Sundermann, *J. Chem. Phys.* **2001**, *114*, 3408–3420.
[36] T. H. Dunning Jr., *J. Chem. Phys.* **1989**, *90*, 1007–1023.
[37] A. E. Reed, L. A. Curtiss, F. Weinhold, *Chem. Rev.* **1988**, *88*, 899–926.
[38] M. J. Frisch, G. W. Trucks, H. B. Schlegel, G. E. Scuseria, M. A. Robb, J. R. Cheeseman, J. A. Montgomery Jr., T. Vreven, K. N. Kudin, J. C. Burant, J. M. Millam, S. S. Iyengar, J. Tomasi, V. Barone, B. Mennucci, M. Cossi, G. Scalmani, N. Rega, G. A. Petersson, H. Nakatsuji, M. Hada, M. Ehara, K. Toyota, R. Fukuda, J. Hasegawa, M. Ishida, T. Nakajima, Y. Honda, O. Kitao, H. Nakai, M. Klene, X. Li, J. E. Knox, H. P. Hratchian, J. B. Cross, C. Adamo, J. Jaramillo, R. Gomperts, R. E. Stratmann, O. Yazyev, A. J. Austin, R. Cammi, C. Pomelli, J. W. Ochterski, P. Y. Ayala, K. Morokuma, G. A. Voth, P. Salvador, J. J. Dannenberg, V. G. Zakrzewski, S. Dapprich, A. D. Daniels, M. C. Strain, O. Farkas, D. K. Malick, A. D. Rabuck, K. Raghavachari, J. B. Foresman, J. V. Ortiz, Q. Cui, A. G. Baboul, S. Clifford, J. Cioslowski, B. B. Stefanov, G. Liu, A. Liashenko, P. Piskorz, I. Komaromi, R. L. Martin, D. J. Fox, T. Keith, M. A. Al-Laham, C. Y. Peng, A. Nanayakkara, M. Challacombe, P. M. W. Gill, B. Johnson, W. Chen, M. W. Wong, C. Gonzalez, J. A. Pople, *Gaussian 03, Revision B.05*, Gaussian, Inc., Pittsburgh PA, **2003**.
[39] G. M. Sheldrick, *SHEXTL 5.10*, Bruker AXS, Inc. Madison. WI. USA, **1998**.
[40] *SADABS: Area-Detector Absorption Correction Programme*, Siemens Industrial Automation, Inc. Madison, WI, **1996**.
[41] CCDC-605842, -605843, -605840, -605841, -605844 contain the supplementary crystallographic data for this paper. These data can be obtained free of charge from The Cambridge Crystallographic Data Centre via www.ccdc.cam.ac.uk/data_request/cif

Received: May 8, 2006